iScience, Volume *26*

Supplemental information

Identification of SIRT3 as an eraser of H4K16la

Zhuming Fan, Zhiyang Liu, Nan Zhang, Wenyu Wei, Ke Cheng, Hongyan Sun, and Quan Hao

Contents

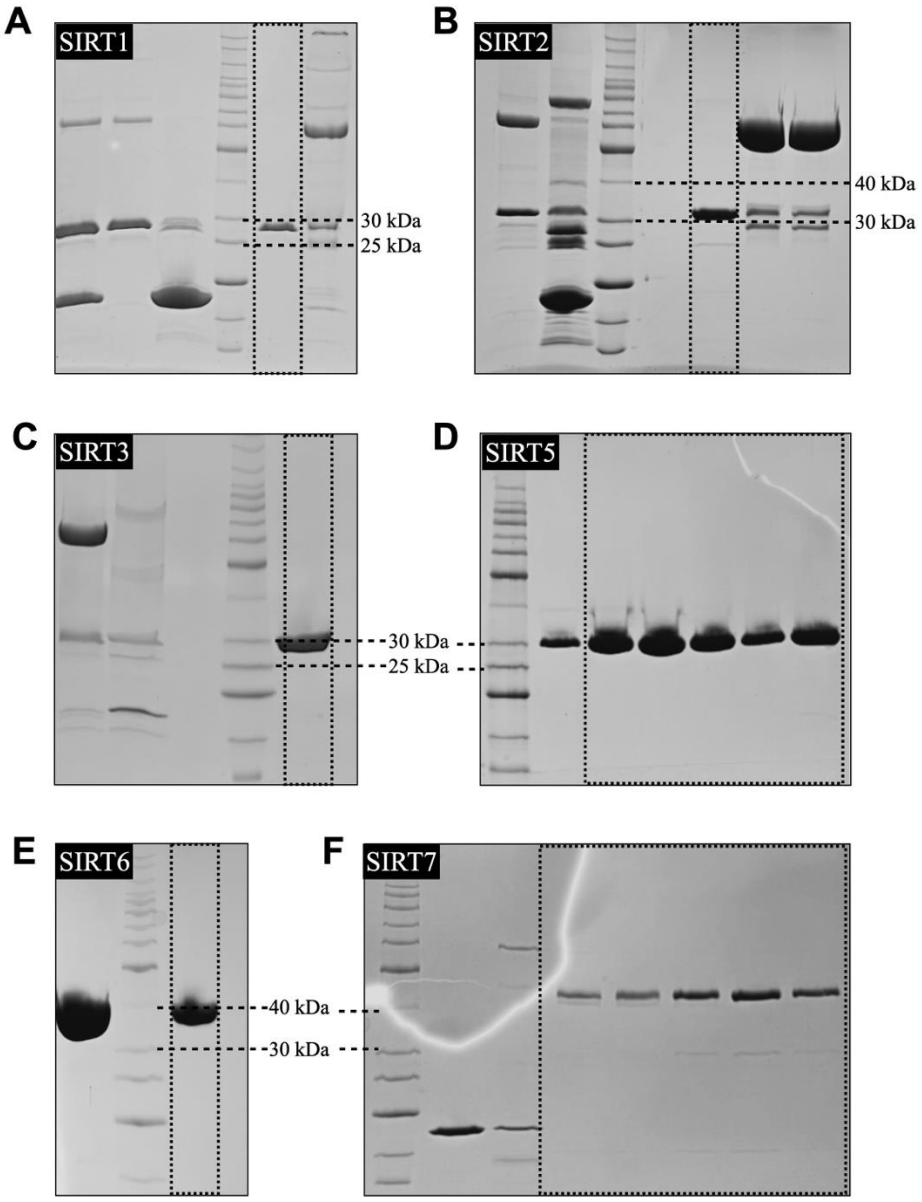

Figure S1. Final purification results of recombinant human Sirtuins, related to Figure 1

hSIRT1 core region (234-505 aa, 30.1 kDa). (B) SIRT2 (50-356 aa, 34.6 kDa). (C) SIRT3 (118-399 aa, 31.2 kDa). (D) SIRT5 (32-302, 29.5 kDa). (E) Full-length SIRT6 (39.1 kDa). (F) Full-length SIRT7 (44.9 kDa). Dot-framed pure fractions were collected, buffer exchanged and concentrated for the following enzymatic and crystallographic experiments.

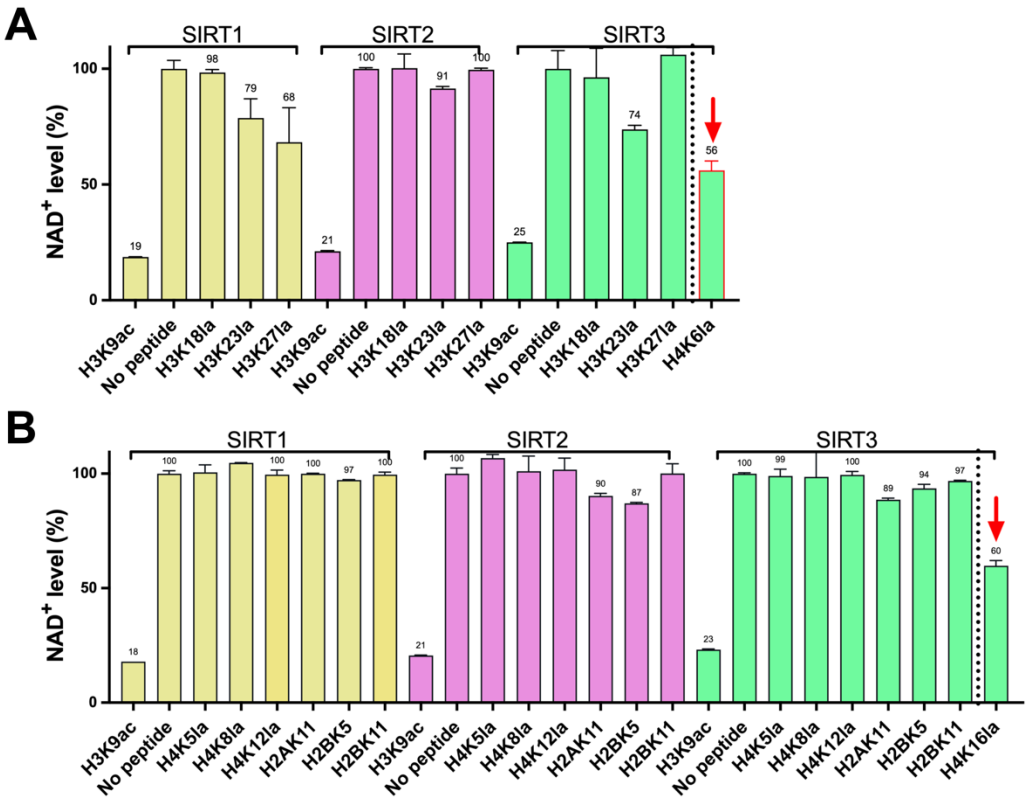

Figure S2. NAD⁺ consumption/cycling assay, related to Figure 1A

(A) 3 h NAD⁺ consumption/cycling assay of SIRT1-3 on H3K18la, H3K23la, H3K27la and H4K16la (SIRT3 only); (B) 3 h NAD⁺ consumption/cycling assay of SIRT1-3 on H4K5la, H4K8la, H4K12la, H2AK11la, H2BK5la, H2BK11la, and H4K16la (SIRT3 only).

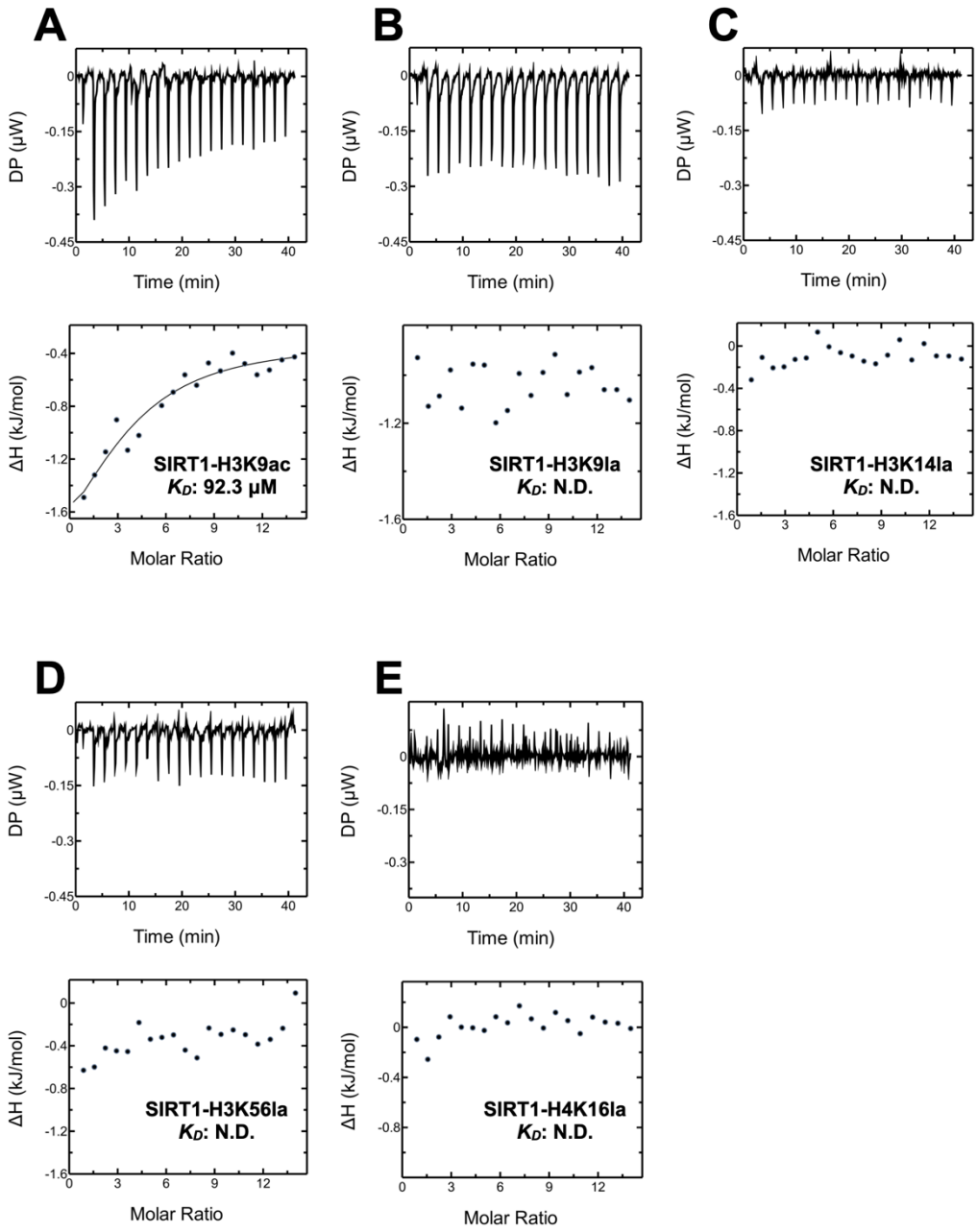

Figure S3. ITC results of SIRT1 with different Kla peptides, related to Figure 1C

40 μL, 2 mM of H3K9ac as the positive control (A), H3K9la (B), H3K14la (C), H3K56la (D) and H4K16la (E) were divided into 20 injections titrated into 200 μL, 30 μM of SIRT1. ITC data and binding affinity were analyzed by MicroCal PEAQ-ITC analysis software.

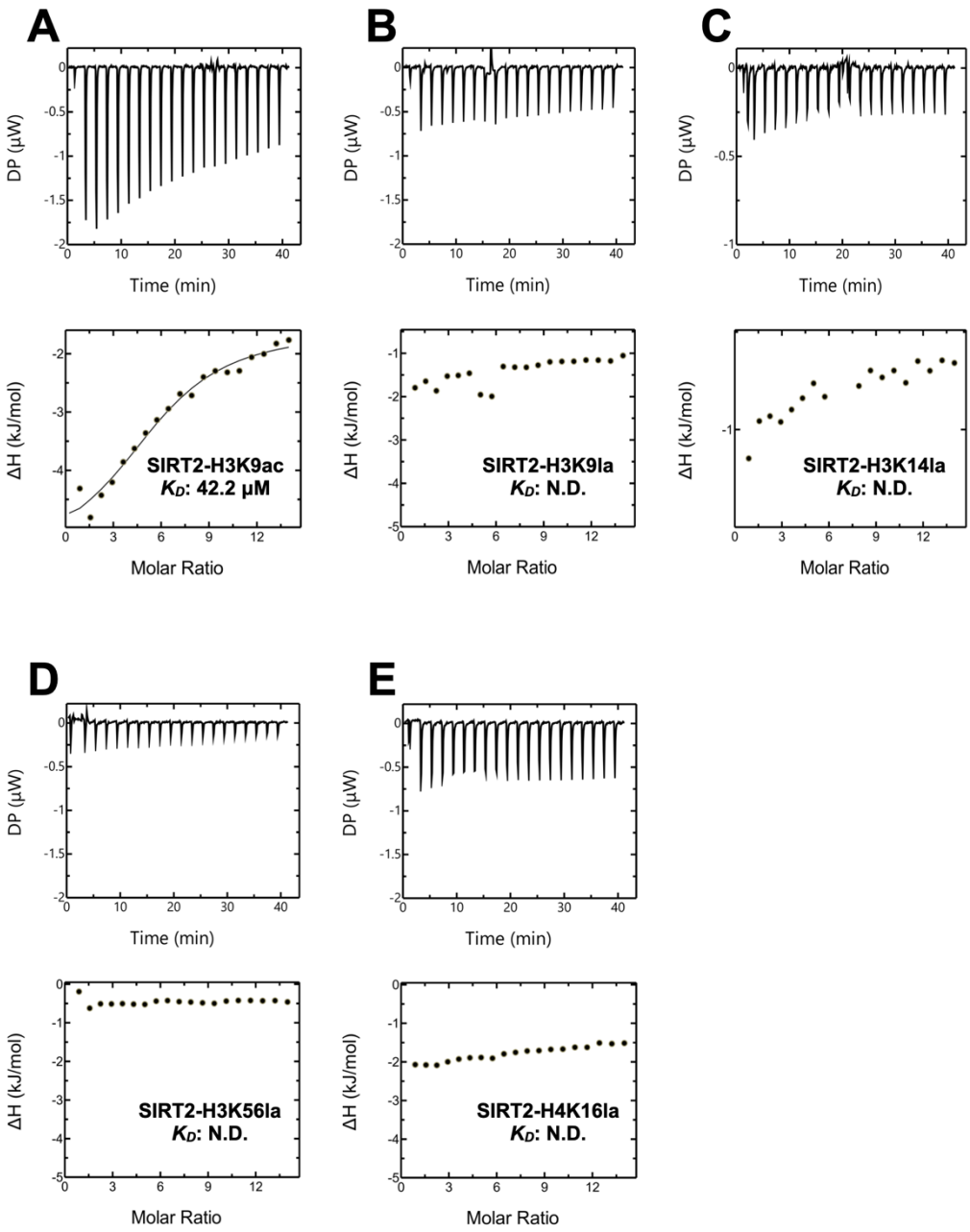

Figure S4. ITC results of SIRT2 with different Kla peptides, related to Figure 1C

40 μL, 2 mM of H3K9ac as the positive control (A), H3K9la (B), H3K14la (C), H3K56la (D) and H4K16la (E) were divided into 20 injections titrated into 200 μL, 30 μM of SIRT2. ITC data and binding affinity were analyzed by MicroCal PEAQ-ITC analysis software.

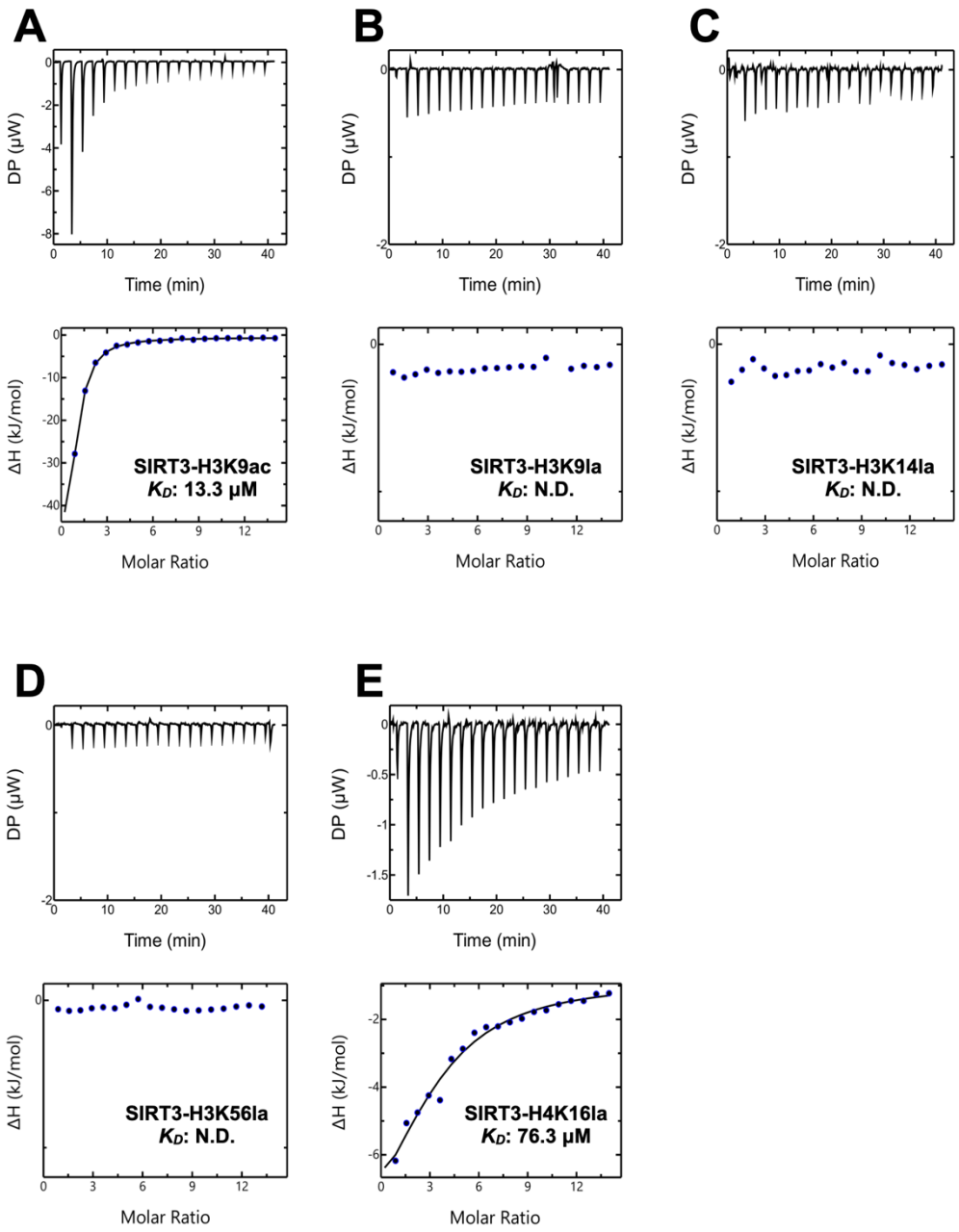

Figure S5. **ITC results of SIRT3 with different Kla peptides, related to Figure 1C**
40 μL, 2 mM of H3K9ac as the positive control (A), H3K9la (B), H3K14la (C), H3K56la (D) and H4K16la (E) were divided into 20 injections titrated into 200 μL, 30 μM of SIRT3. ITC data and binding affinity were analyzed by MicroCal PEAQ-ITC analysis software.

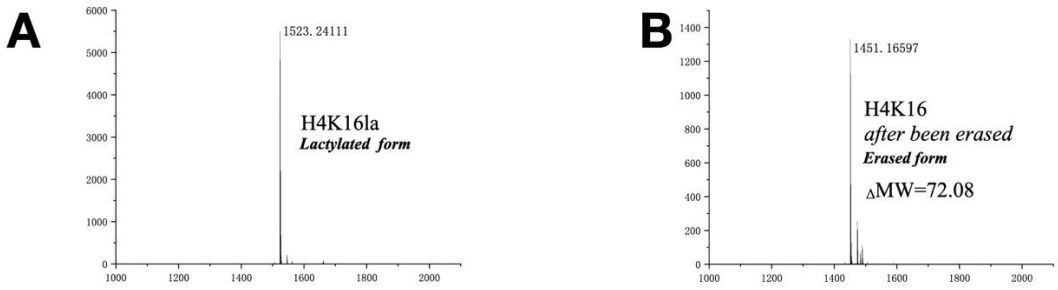

Figure S6. The mass spectrum results for HPLC analysis after incubating Sirtuins and HDAC3 (200 nM) with 100 μM H4K16la, related to Figure 1D, E

(A)H4K16la, (B)H4K16 (modification after being erased). HPLC condition: peptide, 100 μM; protein, 200 nM; 30-100% ACN 3-30 min. The column used: C18-Pro, 4.6x250 mm, 5 μm, 300 Å, J&K Scientific.

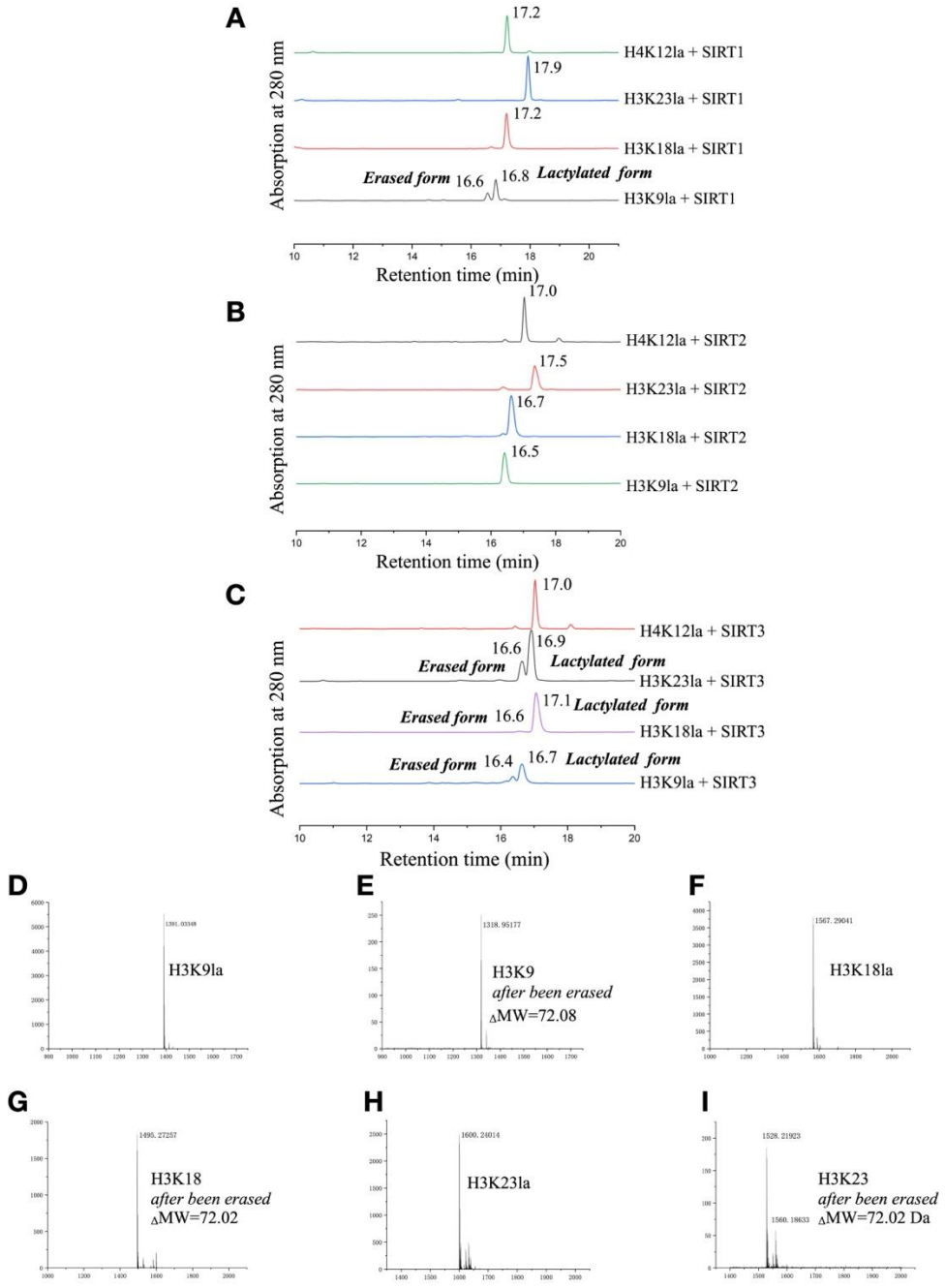

Figure S7. LC-MS analysis for SIRT1-3 and lactyl peptides, related to Figure 1

(A) Comparison of the SIRT1 erasing capacity against H3K9la, H3K18, H3K23la, and H4K12la. (3 hours incubation) (B) Comparison of the SIRT2 erasing capacity against H3K9la, H3K18, H3K23la, and H4K12la. (3 hours incubation) (C) Comparison of the SIRT3 erasing capacity against H3K9la, H3K18, H3K23la, and H4K12la. (3 hours incubation) (D-I) The mass result of H3K9la, H3K18, and H3K23la and their modification-erased form. HPLC condition: peptide, 100 μM; protein, 200 nM; 3-100% ACN 3-20 min. The column used: C18-Pro, 4.6x250 mm, 5 μm, 300 Å, J&K Scientific.

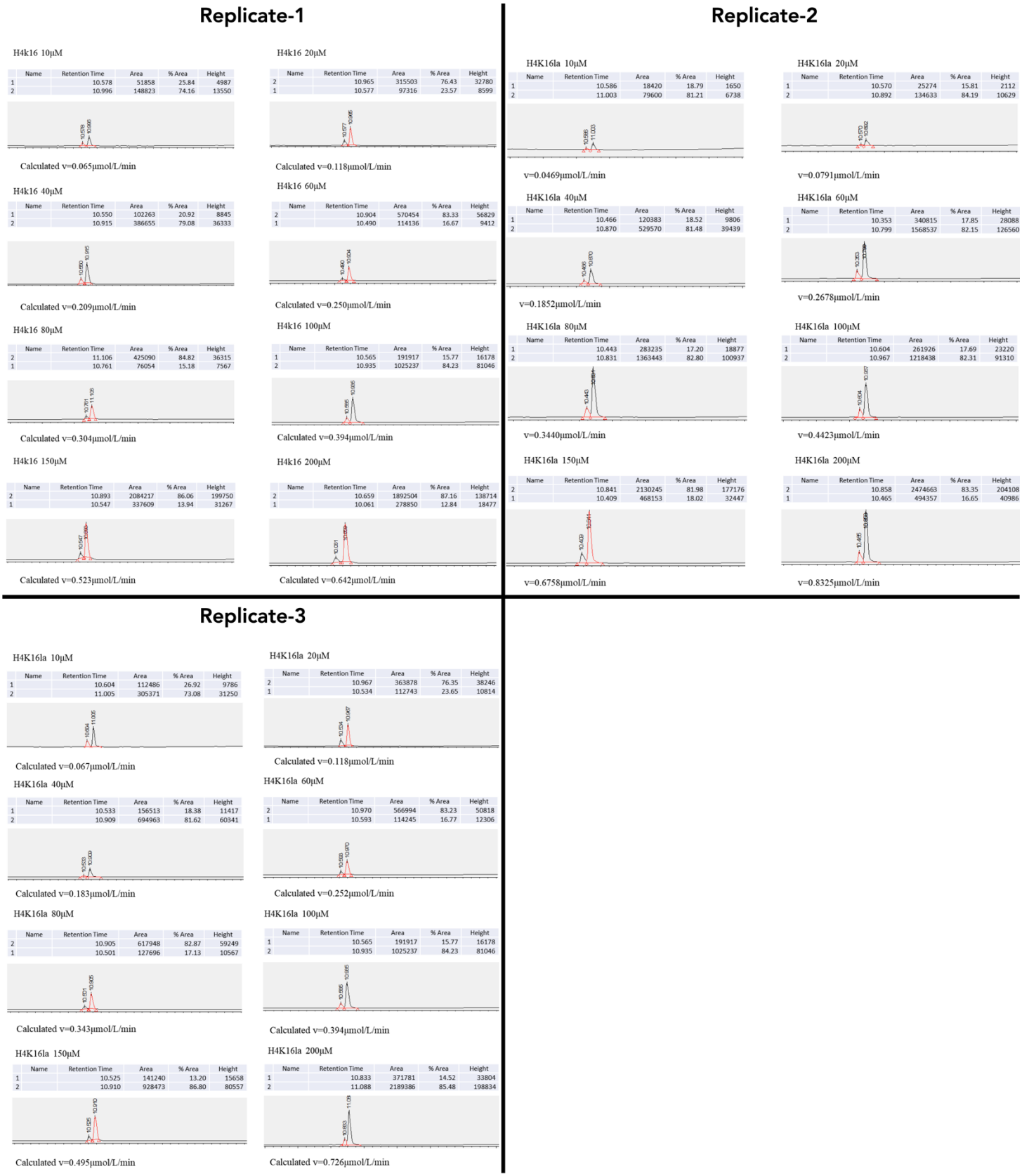

Figure S8. 3 replicates of HPLC analysis results for erasing rate determination, related to Figure 1F

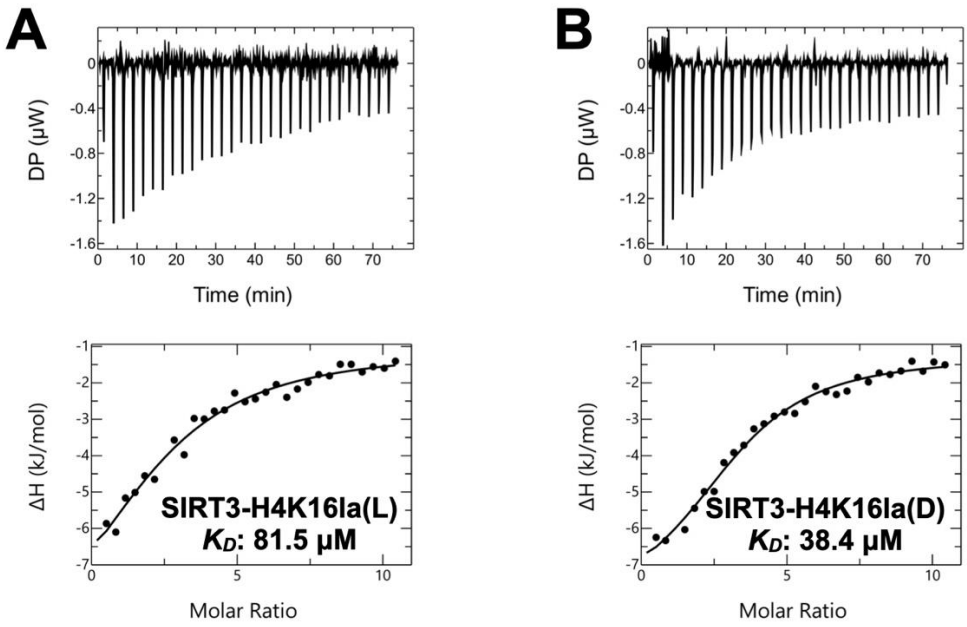

Figure S9. ITC row data of SIRT3 titrated by L(A)/D(B)-H4K16la, related to Figure 1H
ITC data and binding affinity were analyzed by MicroCal PEAQ-ITC analysis software.

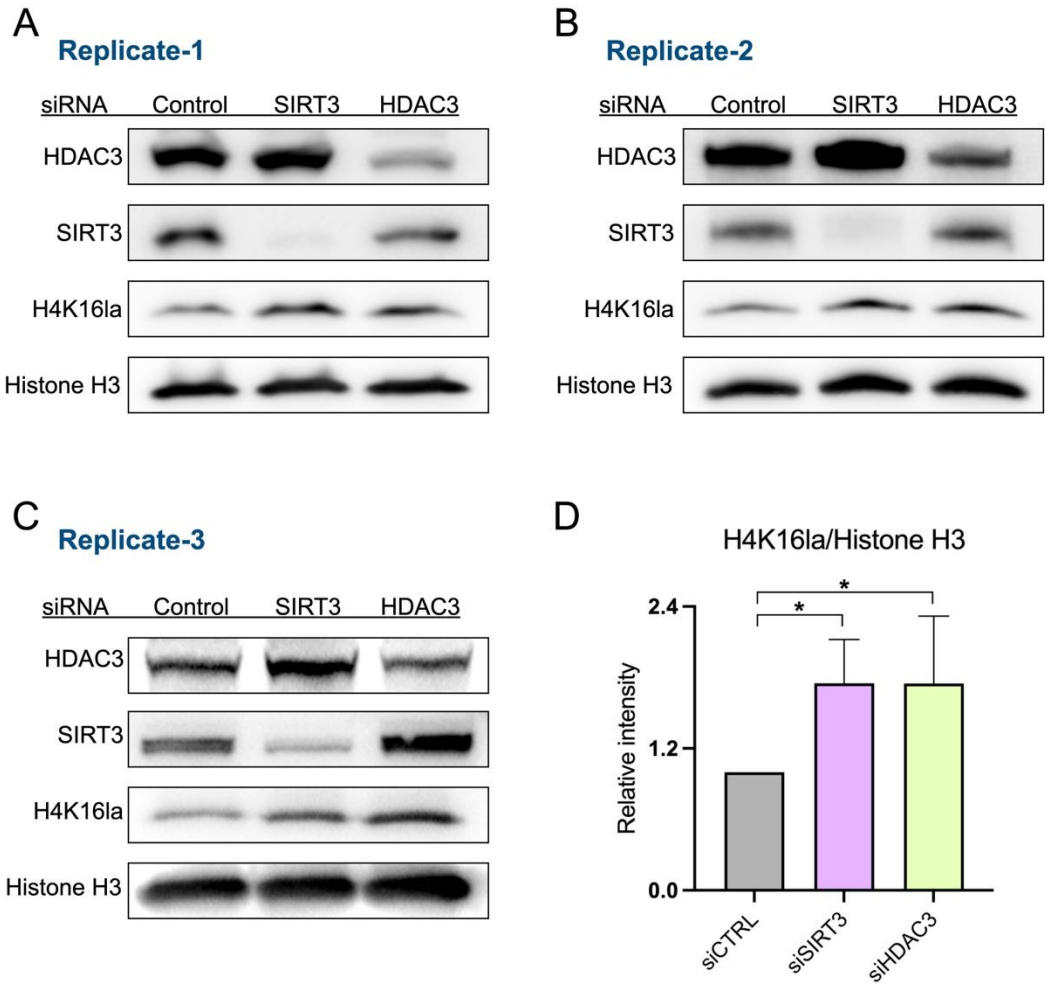

Figure S10. Western blot analysis of cellular H4K16la level change, related to Figure 1I

After 48 h post-knockdown of SIRT3 and HDAC3 via siRNA in HEK293T cells, increased H4K16la level was detected. (A-C) 3 western blot replicates of this experiment. (D) Histone H3 was used as the loading control. Values represent mean ± SD. Statistical comparisons between groups were analyzed using the Student *t* test. **p*<0.05.

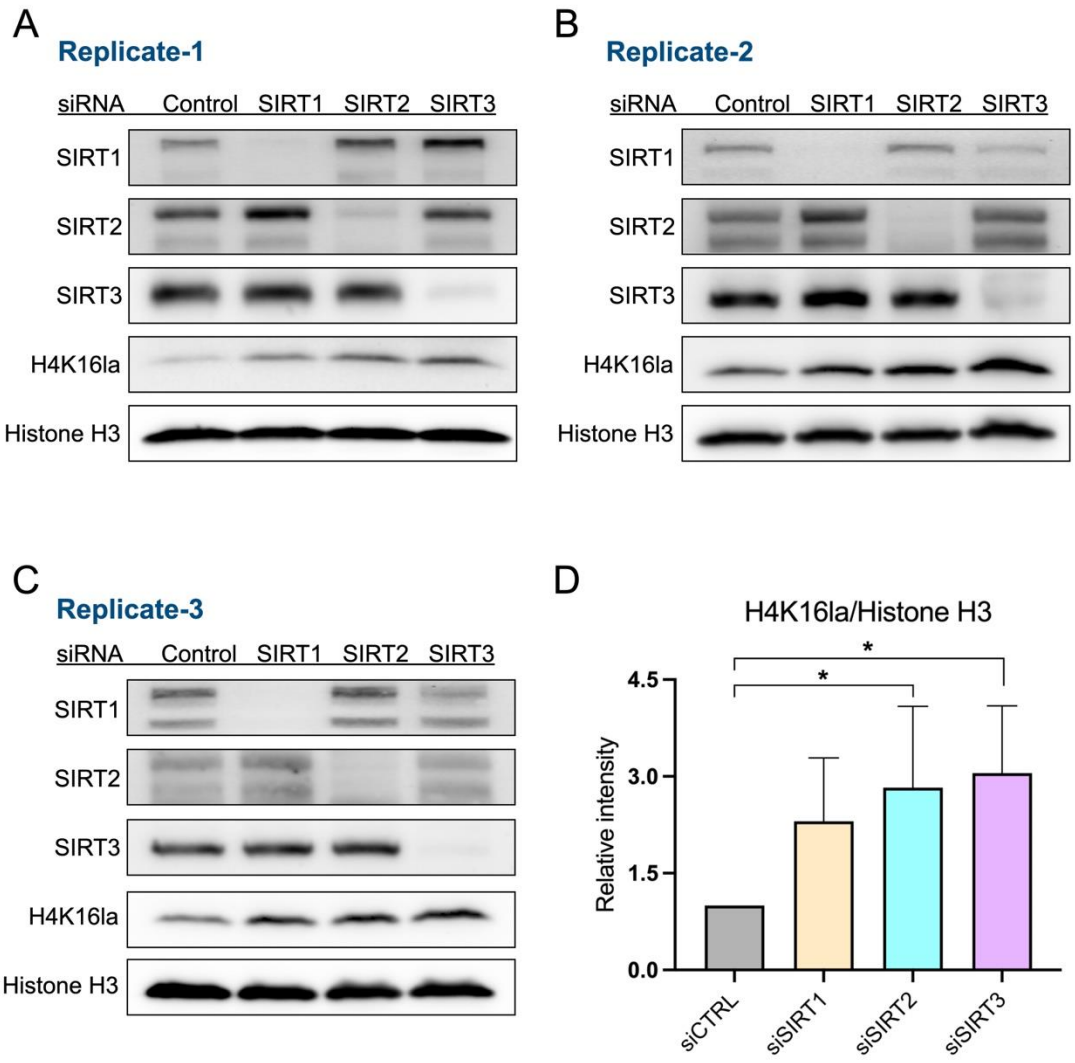

Figure S11. Western blot analysis of cellular H4K16la level change, related to Figure 1J

After 48 h post-knockdown of SIRT1-3 via siRNA in HEK293T cells, increased H4K16la level was detected. (A-C) 3 western blot replicates of this experiment. (D) Histone H3 was used as the loading control. Values represent mean ± SD. Statistical comparisons between groups were analyzed using the Student *t* test. **p*<0.05.

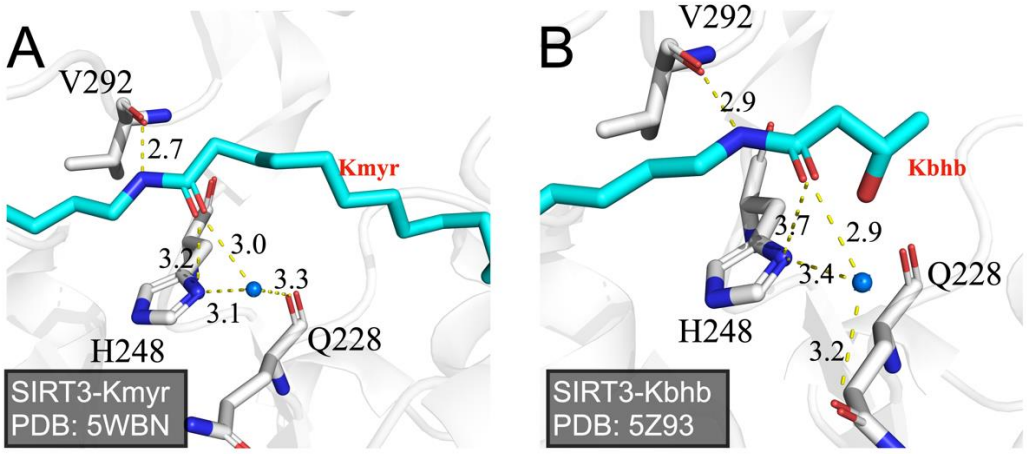

Figure S12. The amido linkage binding details of acyl-lysine with SIRT3, related to Figure 2

(A) PDB 5WBN, SIRT3 in complex with Kmyr peptide. (B) PDB 5Z93, SIRT3 in complex with Kbhb peptide. SIRT3 (grey), acyl-lysine peptides (cyan), water (marine sphere). Hydrogen bond is represented as a dashed line. The length (Å) of the hydrogen bond is labelled next to the dashed line.

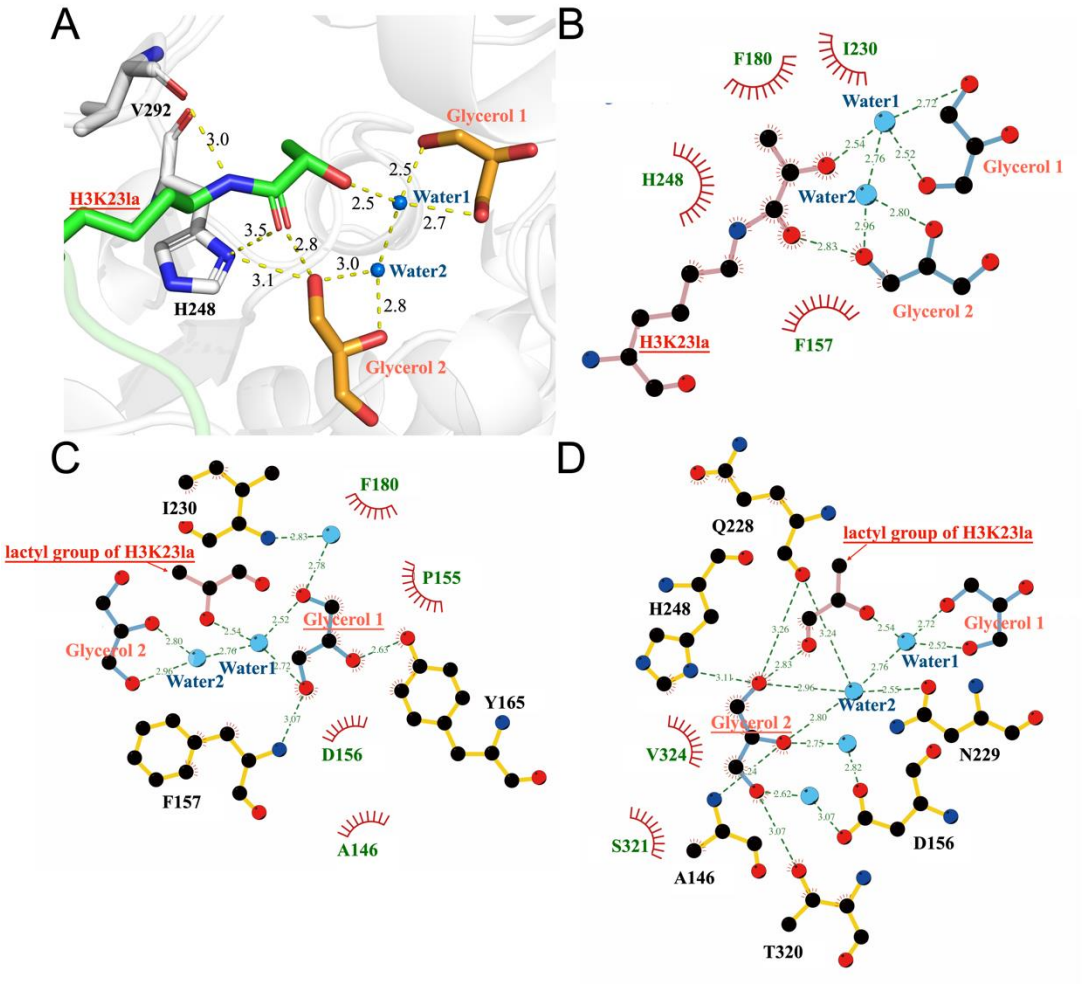

Figure S13. Detailed interactions in SIRT3-H3K23la structure, related to Figure 2

(A) Structure depicting details of the interaction between SIRT3 (white), H3K23la(L) (green), water molecules (marine spheres) and glycerol molecules (orange). (B-D) LIGPLOT diagram describing interactions of surrounding residues and molecules towards the (B) H3K23(L) ligand, (C) glycerol molecule 1 (Glycerol 1) and (D) glycerol molecule 2 (Glycerol 2). H3K23la(L) (bond colour: light pink), glycerol molecules (bond colour: blue) and SIRT3 (bond colour: gold) are depicted in ball-and-stick mode. Carbon is represented as a black ball; nitrogen is represented as a blue ball; oxygen is represented as a red ball; water molecule is represented as a marine sphere; hydrophobic interactions are shown as red arcs; hydrogen bond is represented as a dashed line. The length (Å) of the hydrogen bond is labelled next to the dashed line.

Figure S14. Chemical structure of the lactate probe (alkynyl-labelled mimics), related to Figure 3

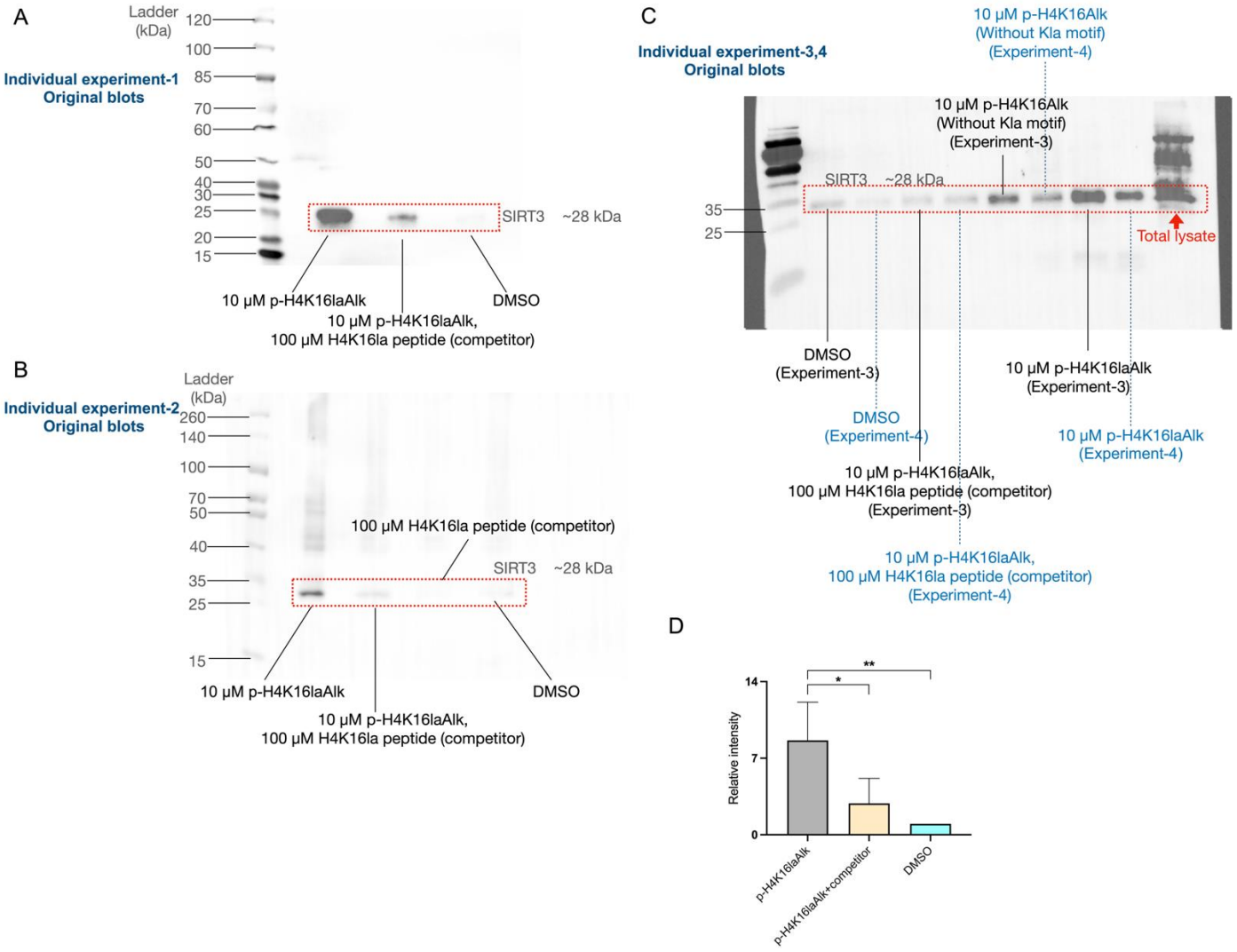

Figure S15. 4 individual experiments of Western blot analysis of detecting the existence of SIRT3 in the pull-down products, related to Figure 3C

(A) Experiment-1: western blot analysis of detecting the existence of SIRT3 in the pull-down products of group$_{\text{p-H4K16laAlk,}}$ group$_{\text{p-H4K16laAlk with competitor}}$, and DMSO group (negative control). (B) Experiment-2: western blot analysis of detecting the existence of SIRT3 in the pull-down products of group$_{\text{p-H4K16laAlk,}}$ group$_{\text{p-H4K16laAlk with competitor}}$, group$_{\text{competitor}}$, and DMSO group (negative control). (C) Experiment-3, 4: western blot analysis of detecting the existence of SIRT3 in the pull-down products of DMSO group (negative control), group$_{\text{p-H4K16laAlk with competitor}}$, group$_{\text{p-H4K16Alk}}$ (probe without lactylation modification), and group$_{\text{p-H4K16laAlk}}$. (D) Values represent mean ± SD. Statistical comparisons between groups were analyzed using the Student *t* test. **p*<0.05, ***p*<0.01.

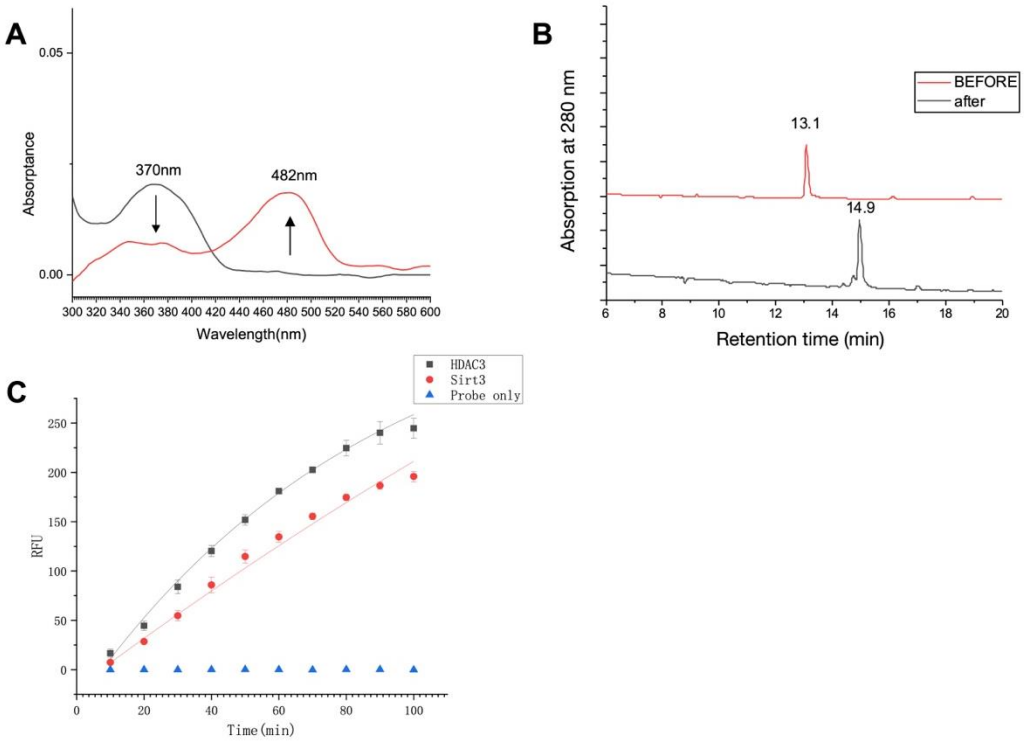

Figure S16. Flurogenic parameter of the p-H4k16laNBD probe, related to Figure 3

(A) Absorption spectra of p-H4K16laNBD probe (10 μM) before (grey) and after (red) enzymatic reaction with SIRT3 (0.2 μM) in 20 mM HEPES buffer (pH = 8.0) containing 100 μM NAD^+ at 37 °C for 2 h. (B) HPLC analysis of the enzymatic reaction of p-H4K16laNBD probe (10 μM) with recombinant SIRT3 (0.2 μM) in 20 mM HEPES buffer (pH = 8.0) containing 100 μM NAD^+ at 37°C for 2 h. (C) Time-dependent fluorescence measurements of p-H4K16laNBD (10 μM) in the presence of HDAC3 (grey) and SIRT3/NAD^+ (red) (λex = 480 nm; λem = 550 nm). The first-order rate constant k of enzymatic reaction is 0.0102 min^{-1} and 0.0059 min^{-1}.

p-H4K16laAlk

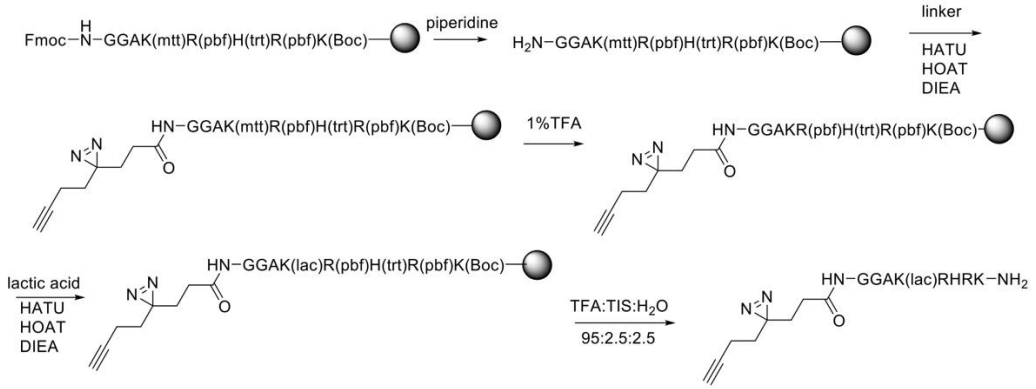

Competitor (H4K16la peptide)

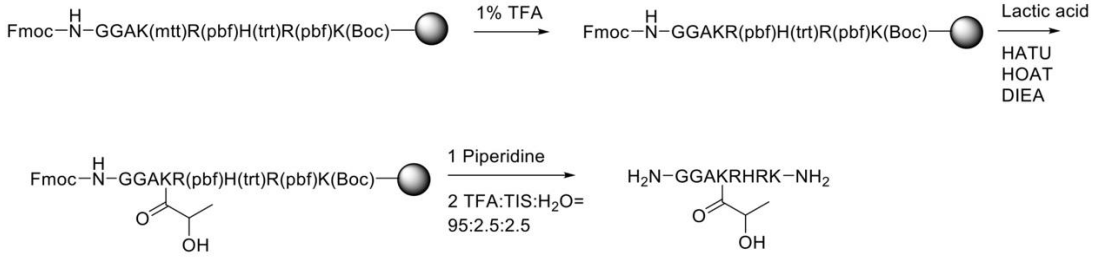

Figure S17. Synthesis procedure of the p-H4K16laAlk (upper) and the competitor (H4K16la peptide) (lower), related to STAR Methods

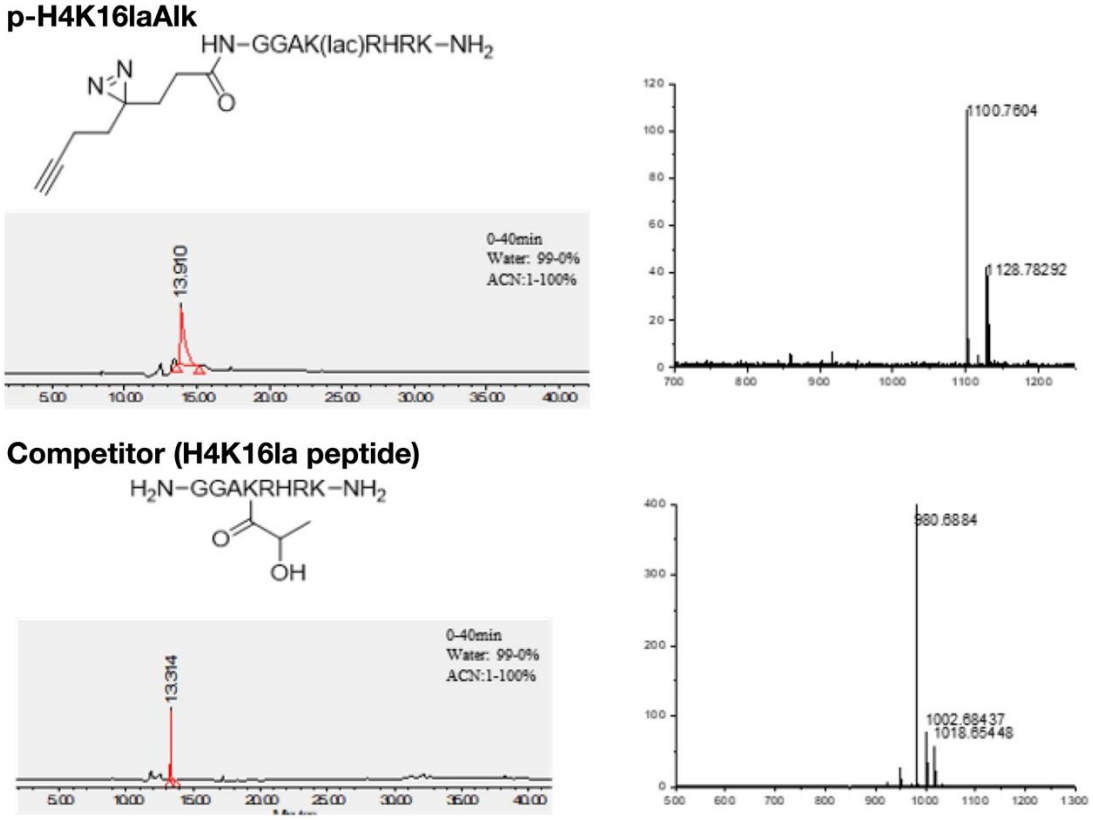

Figure S18. LC-MS analysis of the p-H4K16laAlk (upper) and the competitor (H4K16la peptide) (lower), related to STAR Methods

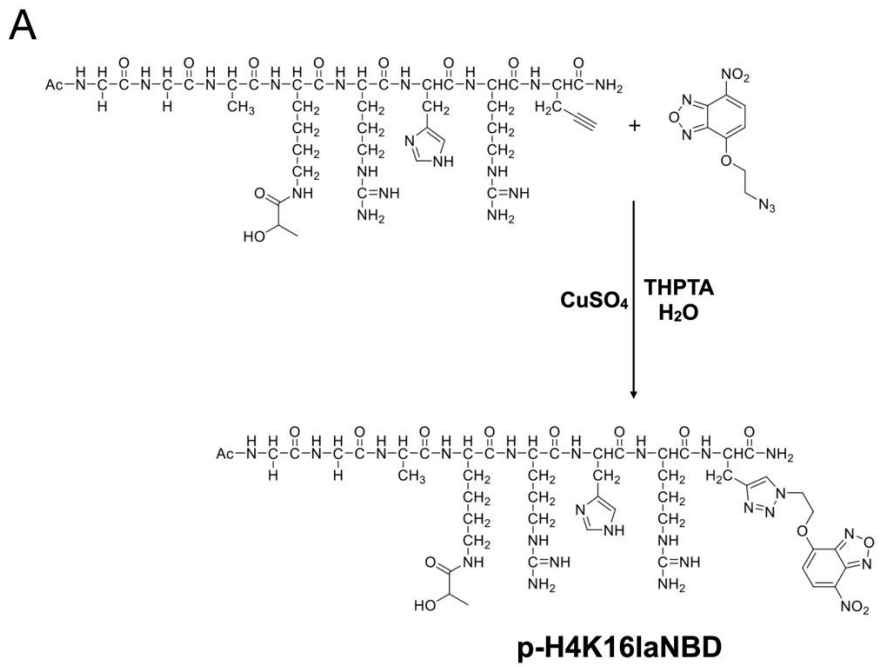

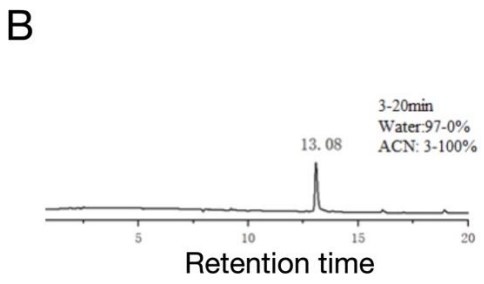

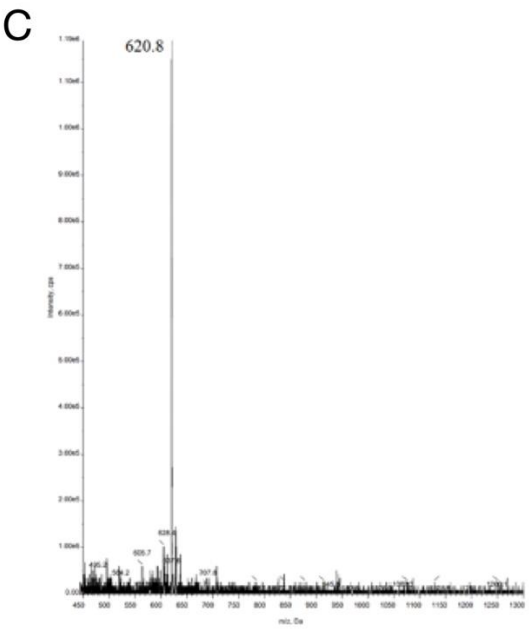

Figure S19. Synthesis procedure and the LC-MS analysis of p-H4K16laNBD, related to STAR Methods

(A) To synthesize p-H4K16laNBD, the peptide sequence Ac-GGAK(lac)RHRPro-NH_2 was synthesized using solid based method. After the purification, the peptide was clicked with N_3-ONBD to give the final probe p-H4K16laNBD.The reaction was conducted for 6 h with strong stirring under the catalyst of Cu(I). (B)(C) The probe was purified and verified by LC-MS.

Table S1. The literature evidence of Sirtuins' preferred sites, related to Figure 1A

Histone site	Sirtuins	Modification types	Description (Sirtuin-histone-acyl-lysine complex structures published from PDB or mentioned in published articles)
H3K9	SIRT1	Ac	SIRT1 binds to H3K9 within the P53 region, and result in decreased H3K9ac level and repressed p53 gene transcription.[1]
	SIRT2	Myr	Published PDB: SIRT2-H3K9myr (4Y6L).[2]
	SIRT3	Pal/Myr/Bhb	Published PDB data: SIRT3-H3K9pal (5BWO) /myr (5BWN)/bhb (5Z93).[3]
	SIRT5	Suc	Published PDB: SIRT5-H3K9suc (3RIY).[4]
	SIRT6	Myr	Published PDB: SIRT6-H3K9myr (3ZG6).[5]
H3K14	SIRT1	Ac	SIRT1 regulate gene expression of HIF-1α via deacetylation on H3K14.[6]
	SIRT2	Ac	Reduced SIRT2 expression caused upregulated H3K14ac level in diabetic cartilage.[7]
	SIRT3	Ac/Bhb	Overexpression of SIRT3 reduced H3K14ac level[8], and SIRT3 is able to de-β-hydroxybutyrylate H3K14 *in vitro*.[9]
H3K56	SIRT1	Ac	SIRT1 binds to H3K56 within the bclaf1 promoter region, and result in decreased H3K56ac level, suppressed bclaf1 expression and inhibited T cell activation.[10]
	SIRT2	Ac	Reduced SIRT2 expression caused upregulated H3K56ac level in diabetic cartilage.[7]
	SIRT3	Ac	Overexpression of SIRT3 reduced H3K56ac level.[8]
	SIRT6	Ac	Deacetylase activity *in vitro*.[11]
H4K16	SIRT1	Ac	SIRT1 represses transcription of TNF-α in THP-1 macrophages via deacetylation on H4K16.[12,13]
	SIRT2	Ac	SIRT2 regulate mitosis via deacetylation on H4K16.[14]
	SIRT3	Bhb	Published PDB: SIRT3-H4K16bhb (5ZGC).[9]
	SIRT5	Ac	SIRT5 deacetylates H4K16ac and regulate the transcription of PDX1.[15]
	SIRT6	Ac	SIRT6 deacetylates H4K16ac and regulate oocyte meiosis.[16]

Table S2. The literature evidence of the nuclear existence of SIRT3, related to Figure 1I, J

SIRT3 type	Cell type	Methods	Conclusion
C-term EGFP labeled SIRT3[9]	HEK293	Colocalization (Z-stack 3D imaging) (DAPI and Anti-EGFP antibody)	C-term EGFP-labeled SIRT3 fluorescence signals in nucleus.
Overexpressed or endogenous SIRT3[9]	HEK293	Cell fractionation study (Western blot))	Overexpressed or endogenous SIRT3 exist in nuclear fractions.
Endogenous SIRT3[9]	HEK293	bhbNa treatment (Western blot))	SIRT3 level increased in chromatin-bound fractions when histone Kbhb level upregulated.
SIRT3 knockdown [17]	Hela	si-RNA knockdown (Western blot)	SIRT3 knockdown caused upregulated pan-Kcr and H3K4cr level
Endogenous SIRT3[17]	Hela	Colocalization (DAPI and anti-SIRT3 N-term antibody)	The full length SIRT3 exists in nucleus.
Endogenous SIRT3[17]	Hela	Cell fractionation study (Western blot)	SIRT3 can be detected in nuclear fractions by using both anti SIRT3 N- and C-term antibodies.
Endogenous SIRT3[18]	HEK293F	Cell fractionation study (Western blot)	SIRT3 (both full length and the processed one lacking N-term 142 amino acids) can be detected in nucleus.
C-term HA tagged SIRT3 (tetracycline induced)[18]	HEK293F	Cell fractionation study (Western blot) and Colocalization (DAPI and anti-SIRT3 N-term antibody)	SIRT3-HA (both full length and the processed one lacking N-term 142 amino acids) can be detected in nucleus.
C-term FLAG tagged SIRT3[19]	HEK293T	Proteomic analysis (Identification of SIRT3 interacting proteins)	Lamin B1 (nuclear envelop protein), and KAP1 (heterochromatin-associated protein) were identified by LC-MS/MS.
C-term FLAG tagged SIRT3[19]	HEK293T	Co-IP (Western blot)	SIRT3 interacts with the nuclear proteins, including Lamin B1, KAP1, HP1α, HP1γ, and LBR.
Endogenous SIRT3[19]	hMSCs	Cell fractionation study (Western blot)	Both SIRT3 and Lamin B1 were detected in nuclear fraction.
C-term FLAG tagged SIRT3 overexpressed in SIRT3$^{-/-}$ hMSCs[19]	hMSCs	Colocalization (Z-stack 3D imaging) (Anti Lamin B1 and Anti-FLAG antibody)	SIRT3 and Lamin B1 colocalized at nucleus.

Table S3. Crystal data collection and refinement statistics, related to Figure 2

Data collection	**(SIRT3-H3K23la)**	**(SIRT3-H4K16la)**
Wavelength (Å)	0.976	0.976
Resolution range (Å)	42.38 - 1.998 (2.07 - 1.998)	45.24 - 2.501 (2.59 - 2.501)
Space group	P 2_1 2_1 2_1	P 6_5
Unit cell	33.043 84.763 89.187 (Å) 90 90 90 (º)	97.449 97.449 53.583 (Å) 90 90 120 (º)
Total reflections	25417 (1294)	19276 (1630)
Unique reflections	16948 (1273)	10160 (994)
Multiplicity	1.5 (1.0)	1.9 (1.6)
Completeness (%)	95.93 (72.33)	99.79 (98.61)
Mean I/sigma (I)	15.12 (3.48)	28.75 (4.26)
Wilson B-factor	22.99	33.42
R-merge	0.03378 (0.07989)	0.03693 (0.1884)
R-meas	0.04777 (0.113)	0.05222 (0.2665)
R-pim	0.03378 (0.07989)	0.03693 (0.1884)
CC1/2	0.996 (1)	0.996 (0.843)
CC*	0.999 (1)	0.999 (0.956)
Refinement		
Reflections used in Refinement	16948 (1292)	10153 (992)
Reflections used for R-free	1697 (133)	1004 (100)
R-work	0.1570 (0.2149)	0.1877 (0.2366)
R-free	0.2006 (0.2559)	0.2426 (0.3080)
CC (work)	0.954 (0.896)	0.961 (0.844)
CC (free)	0.925 (0.881)	0.938 (0.645)
Number of non-	2370	2281

hydrogen atoms		
macromolecules	2173	2168
ligands	56	6
solvent	169	107
Protein residues	276	274
RMS (bonds)	0.005 (Å)	0.003 (Å)
RMS (angles)	0.78 (º)	0.6 (º)
Ramachandran favored (%)	97.79	97.76
Ramachandran allowed (%)	2.21	2.24
Ramachandran outliers (%)	0.00	0.00
Rotamer outliers (%)	0.00	0.42
Clashscore	2.04	3.67
Average B-factor	27.54	47.05
macromolecules	27.17	46.83
ligands	29.18	39.81
solvent	31.97	51.87
Number of TLS groups	1	1

Statistics for the highest-resolution shell are shown in parentheses.

Table S4. Proteomic analysis: protein identified after enrichment (with enriched ratio≥2, $p < 0.05$), related to Figure 3B

	$Log_2(K_{p\text{-}H4K16laAlk} / K_{p\text{-}H4K16laAlk\ with\ 100\mu M\ competitor})$	-Log(p-value)
SIRT3	3.528473	3.880375
RPL19	2.936674	1.801582
DKC1	2.927341	1.614196
SRSF1	2.686776	1.977218
SRSF7	2.571431	2.023642
GMPS	2.537244	2.094105
RPL10	2.473908	1.513292
RPL18A	2.468427	1.840031
EBNA1BP2	2.413991	2.24365
TOP1	2.311893	1.409809
ARF1	2.270554	2.947051
ATAD3A	2.164889	1.364628
RPL13	2.112772	2.172246
HNRNPH2	2.035472	1.409859
RPL7	1.907576	1.71624
FBL	1.894831	2.483103
RPS3A	1.84828	1.768023
TLN1	1.838418	1.607041
RPL17	1.82833	1.472486
RPL15	1.770842	1.593327
CPT1A	1.75947	4.307828
RPL3	1.691245	1.494277
RPL11	1.63718	1.557138
CSNK2A3;CSNK2A1	1.489653	2.223984
GTPBP4	1.453023	1.442969
RPS6	1.424533	2.46101
LMNA	1.420535	1.937808
TARS	1.40882	1.727108
EIF3A	1.405017	1.682487
HP1BP3	1.390128	1.919034
CLPB	1.386087	1.449422
VDAC3	1.318909	1.480091
MYBBP1A	1.313581	1.768858
RPS8	1.3128	1.441611
ABCD3	1.31063	1.778466
RPS11	1.302059	1.808605
RPS7	1.301185	1.770535
KPNB1	1.289495	2.431653
PABPC4	1.268914	1.421224
NCLN	1.262781	2.141539
SLC25A6;SLC25A4	1.243965	1.423398
RPL8	1.217177	3.47264
MSN	1.211431	2.360911

RFC5	1.192929	1.934166
VDAC1	1.191338	1.404913
RAB2A;RAB2B	1.185791	1.61055
RPL5	1.138686	1.331613
NAT10	1.124737	1.753622
UQCRC2	1.115121	1.353112
RPL18	1.083732	1.474
NPM1	1.051168	1.743963
CACYBP	1.043609	1.38192
HNRNPA1;HNRNPA1L2	1.036201	2.17814
PSMD3	1.032894	1.794367
ACAT1	1.008949	2.449278
RPL4	1.002317	2.250274

Table S5. Peptide sequences used in NAD+ consumption/cycling assay, related to STAR Methods

Lactyl-lysine sites	Sequences
H3K9	QTARK (L/D lactic acid) STGG
H3K14	STGGK (L/D lactic acid) APRK
H3K56	RRYQK (L/D lactic acid) STEL
H4K16	KGGAK (L/D lactic acid) RHRK

Table S6. Peptide sequences used in ITC assay, related to STAR Methods

Lactyl-lysine sites	Sequences
H3K9	QTARK (L/D-lactic acid) STGG
H3K14	STGGK (L/D-lactic acid) APRK
H3K56	RRYQK (L/D-lactic acid) STEL
H4K16	KGGAK (L/D-lactic acid) RHRK
H4K16	KGGAK (L-lactic acid) RHRK
H4K16	KGGAK (D-lactic acid) RHRK

Table S7. Peptide sequences used in HPLC-MS analysis, related to STAR Methods

Lactyl-lysine sites	Sequences
H3K9	WQTARK (L/D-lactic acid) STGGW
H3K18	WKAPPK (L/D-lactic acid) QLATKW
H3K23	WKQLATK (L/D-lactic acid) AARKW
H4K12	WKGLGK (L/D-lactic acid) GGAKW
H4K16	WKGGAK (L/D-lactic acid) RHRKW

Reference

1. Wang, R.-H., Zheng, Y., Kim, H.-S., Xu, X., Cao, L., Lahusen, T., Lee, M.-H., Xiao, C., Vassilopoulos, A., and Chen, W. (2008). Interplay among BRCA1, SIRT1, and Survivin during BRCA1-associated tumorigenesis. Molecular cell *32*, 11-20.
2. Feldman, J.L., Dittenhafer-Reed, K.E., Kudo, N., Thelen, J.N., Ito, A., Yoshida, M., and Denu, J.M. (2015). Kinetic and structural basis for acyl-group selectivity and NAD+ dependence in sirtuin-catalyzed deacylation. Biochemistry *54*, 3037-3050.
3. Gai, W., Li, H., Jiang, H., Long, Y., and Liu, D. (2016). Crystal structures of SIRT 3 reveal that the α2-α3 loop and α3-helix affect the interaction with long-chain acyl lysine. FEBS letters *590*, 3019-3028.
4. Du, J., Zhou, Y., Su, X., Yu, J.J., Khan, S., Jiang, H., Kim, J., Woo, J., Kim, J.H., and Choi, B.H. (2011). Sirt5 is a NAD-dependent protein lysine demalonylase and desuccinylase. Science *334*, 806-809.
5. Jiang, H., Khan, S., Wang, Y., Charron, G., He, B., Sebastian, C., Du, J., Kim, R., Ge, E., and Mostoslavsky, R. (2013). SIRT6 regulates TNF-α secretion through hydrolysis of long-chain fatty acyl lysine. Nature *496*, 110-113.
6. Dong, S.-Y., Guo, Y.-J., Feng, Y., Cui, X.-X., Kuo, S.-H., Liu, T., and Wu, Y.-C. (2016). The epigenetic regulation of HIF-1α by SIRT1 in MPP+ treated SH-SY5Y cells. Biochemical and biophysical research communications *470*, 453-459.
7. Qu, Z., Ma, X., Huang, S., Hao, X., Li, D., Feng, K., and Wang, W. (2020). SIRT2 inhibits oxidative stress and inflammatory response in diabetic osteoarthritis. Eur Rev Med Pharmacol Sci *24*, 2855-2864.
8. Palomer, X., Román-Azcona, M.S., Pizarro-Delgado, J., Planavila, A., Villarroya, F., Valenzuela-Alcaraz, B., Crispi, F., Sepúlveda-Martínez, Á., Miguel-Escalada, I., and Ferrer, J. (2020). SIRT3-mediated inhibition of FOS through histone H3 deacetylation prevents cardiac fibrosis and inflammation. Signal transduction and targeted therapy *5*, 1-10.
9. Zhang, X., Cao, R., Niu, J., Yang, S., Ma, H., Zhao, S., and Li, H. (2019). Molecular basis for hierarchical histone de-β-hydroxybutyrylation by SIRT3. Cell discovery *5*, 1-15.
10. Kong, S., Kim, S.-J., Sandal, B., Lee, S.-M., Gao, B., Zhang, D.D., and Fang, D. (2011). The type III histone deacetylase Sirt1 protein suppresses p300-mediated histone H3 lysine 56 acetylation at Bclaf1 promoter to inhibit T cell activation. Journal of Biological Chemistry *286*, 16967-16975.
11. Kokkonen, P., Rahnasto-Rilla, M., Mellini, P., Jarho, E., Lahtela-Kakkonen, M., and Kokkola, T. (2014). Studying SIRT6 regulation using H3K56 based substrate and small molecules. European Journal of Pharmaceutical Sciences *63*, 71-76.
12. Chen, G.D., Yu, W.D., and Chen, X.P. (2016). SirT1 activator represses the transcription of TNF-α in THP-1 cells of a sepsis model via deacetylation of H4K16. Molecular Medicine Reports *14*, 5544-5550.
13. Hajji, N., Wallenborg, K., Vlachos, P., Füllgrabe, J., Hermanson, O., and Joseph, B. (2010). Opposing effects of hMOF and SIRT1 on H4K16 acetylation and the sensitivity to the topoisomerase II inhibitor etoposide. Oncogene *29*, 2192-2204.
14. Vaquero, A., Scher, M.B., Lee, D.H., Sutton, A., Cheng, H.-L., Alt, F.W., Serrano, L., Sternglanz, R., and Reinberg, D. (2006). SirT2 is a histone deacetylase with preference for

histone H4 Lys 16 during mitosis. Genes & development *20*, 1256-1261.

15. Ma, Y., and Fei, X. (2018). SIRT5 regulates pancreatic β-cell proliferation and insulin secretion in type 2 diabetes. Experimental and therapeutic medicine *16*, 1417-1425.
16. Han, L., Ge, J., Zhang, L., Ma, R., Hou, X., Li, B., Moley, K., and Wang, Q. (2015). Sirt6 depletion causes spindle defects and chromosome misalignment during meiosis of mouse oocyte. Scientific reports *5*, 1-10.
17. Xiucong, B., Yi, W., Xin, L., Xiao-Meng, L., Zheng, L., Tangpo, Y., Fat, W.C., Jiangwen, Z., Quan, H., and David, L.X. (2014). Identification of 'erasers' for lysine crotonylated histone marks using a chemical proteomics approach. eLife,3,(2014-10-07) *3*.
18. Scher, Michael, B., Vaquero, Alejandro, Reinberg, and Danny (2007). SirT3 is a nuclear NAD⁺-dependent histone deacetylase that translocates to the mitochondria upon cellular stress. Genes & Development.
19. Diao, Z., Ji, Q., Wu, Z., Zhang, W., Cai, Y., Wang, Z., Hu, J., Liu, Z., Wang, Q., and Bi, S. (2021). SIRT3 consolidates heterochromatin and counteracts senescence. Nucleic Acids Research.